Refereed Proceedings

The 13th International Conference on Fluidization - New Paradigm in Fluidization Engineering

Engineering Conferences International *Year* 2010

IMPACT BEHAVIOUR OF PARTICLES WITH LIQUID FILMS: ENERGY DISSIPATION AND STICKING CRITERIA

Sergiy Antonyuk* Stefan Heinrich†

Stefan Palzer‡

*Hamburg University of Technology, antonyuk@tuhh.de

†Hamburg University of Technology

‡Nestlé Research Center Lausanne

IMPACT BEHAVIOUR OF PARTICLES WITH LIQUID FILMS: ENERGY DISSIPATION AND STICKING CRITERIA

Sergiy Antonyuk[1], Stefan Heinrich[1], Stefan Palzer[2]

[1] Hamburg University of Technology, Institute of Solids Process Engineering and Particle Technology, Denickestr. 15, 21073 Hamburg, Germany
Tel.:+49-40-428782748; fax: +49-40-428782678; e-mail: antonyuk@tuhh.de (Sergiy Antonyuk)

[2] Nestlé Research Center Lausanne, Vers-Chez-Les-Blanc, Switzerland

The normal impact of spherical particles (elastic glass, elastic-plastic Al_2O_3) and non-spherical dominantly plastic agglomerates of amorphous maltodextrin on a wall with a liquid layer was studied. The objective was to investigate the effects of thickness (0.1-1 mm) and viscosity of the liquid layer (1-250 mPa·s) as well as of the impact velocity (1-3.0 m/s) of the granule on the restitution coefficient. The restitution coefficient was measured by using a free-fall apparatus. In the presence of a liquid layer, the higher the viscosity and thickness of the liquid layer the more the energy dissipated during impact and the smaller the critical thickness needed for the sticking of the particle. The measured restitution coefficients were compared with experiments performed without liquid layer. In contrast to the dry restitution coefficient, due to viscous losses at lower impact velocity, higher energy dissipation was obtained. A rational explanation for the effects obtained was given by establishing and numerically solving the force and energy balances for particles impacting on a liquid layer. The model takes into account forces acting on the particle, which includes viscous forces, surface tension and capillary forces, contact forces due to deformation of the wall, drag forces, buoyancy and gravity. A good agreement between simulations and experiments has been achieved. The results are essential for estimating the adhesion probability during agglomeration processes and crusting on equipment surfaces.

1. INTRODUCTION

The moisture content in fluidized beds during spray agglomeration shows a great influence on the inter-particle collision properties and hence on the flow and agglomeration behaviour [1]. During this process the most important mechanisms of granule collisional energy loss are the micro processes of coating of the particle surface with a liquid film or droplets and the wetting of the particles [2-3].

During injection of a liquid binder in the granulator liquid films and small droplets on the surface of particles are formed. These can build liquid or viscous bridges during the impact and might lead to sticking of the particles, i.e. their agglomeration. The initial kinetic energy is dissipated due to shear flow of the liquid between particles during impact, extension and rupture of the formed liquid bridges during rebounding [3].

In this work, the influence of thickness of the liquid layer, liquid viscosity and impact velocity on the energy dissipation during normal impact of spherical particles on a wall coated with liquid were analyzed. Based on the measurements and simulations the influence of these parameters on the critical liquid height at which the granule stick to the wall was investigated.

2. FORCE BALANCE OF THE IMPACT

With relation to the forces acting on the particle the impact process can be divided into four intervals (see Fig. 1). In the first period, the particle penetrates into the liquid layer and displaces the liquid in the contact area. The particle-wall contact with a total displacement x_{tot} takes place during the second period. After loss of contact the particle moves upward through the liquid to the liquid surface (third period). During the last period a liquid bridge is formed. This bridge will be stretched up to a critical length $h_{br,max}$, where its rupture occurs.

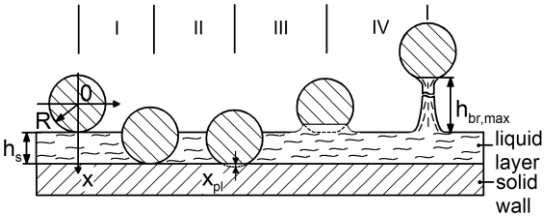

I. Particle penetration: $x \downarrow \in [0;\ h_s]$
II. Particle-wall contact: $x \downarrow \in [h_s;\ h_s+x_{tot}]$
$x \uparrow \in [h_s+x_{tot};\ h_s+x_{pl}]$
III. Emergence of particle: $x \uparrow \in [h_s;\ 0]$
IV. Formation of the liquid bridge: $x \uparrow \in [0;\ -h_{br,max}]$

FIGURE 1. Schematic representation of the different impact phases.

The equation of motion of a particle impacted on the wall with a liquid layer can be expressed as:

$$m_p \ddot{\vec{x}} = \vec{F}_{p,g} + \vec{F}_t + \vec{F}_b + \vec{F}_D + \\ + \vec{F}_c + \vec{F}_{vis} + \vec{F}_{cap} + \vec{F}_{l,g}, \quad (1)$$

with the following forces (see Fig. 2): $F_{p,g}, F_{l,g}$ - gravitational forces of the particle and the liquid film on the particle, F_t - force caused by surface tension, F_b - buoyancy force, F_D - drag force, F_c -contact force between the particle and the wall (force caused by viscoelastic deformation of particle), F_{vis} - viscous force, F_{cap}- capillary force.
The surface tension force F_t was determined for a liquid bridge under static conditions by Orr et al. [4], calculated and measured by many authors [5]-[6] as:

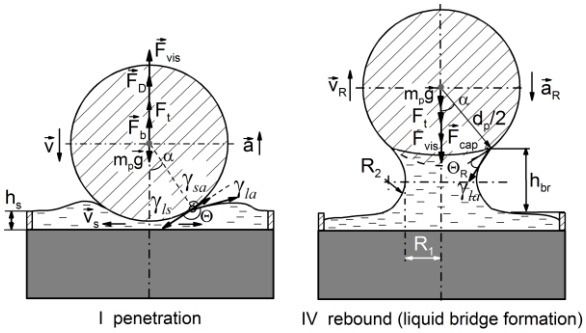

FIGURE 2. Forces acting on the particle during penetration and rebound.

$$F_t = \pm \gamma_{la}\ \pi\, d_p\ \sin\alpha\ \sin(\Theta + \alpha), \quad (2)$$

where γ_{la} is the interfacial tension at the liquid air interface and α is the half of the central angle (Fig. 2). The dynamic contact angle Θ depends on the on the magnitude of the different interfacial tensions and the surface roughness of the particle.

In the investigated cases the buoyancy force is relatively small and can be neglected. The drag force F_D can be calculated by the following equation:

$$F_D = \pm \frac{1}{8} \pi\, c_D\ \rho_l\ d_p^2\ \sin^2(\alpha)\ v^2, \quad (3)$$

where v is the particle velocity and c_D is the drag coefficient which is according to Kaskas [7]:

$c_D = 24/\mathrm{Re} + 4/\sqrt{\mathrm{Re}} + 0.4$, for the Reynolds number range: $0 < \mathrm{Re} < (2\text{-}4)\cdot 10^5$. (4)

During the second phase of impact the granule gets in contact with the wall below the liquid film. The contact force F_c can be expressed as a sum of an elastic force (first term in Eq. (5) according to Hertz [8]) and a damping force (second term in Eq. (5) according to Tsuji [9]):

$$F_c = k'_{el}\, x^{3/2} + \alpha_d \sqrt{m^*\ k'_{el}}\ x^{1/4}\ \frac{dx}{dt} \quad (5)$$

with the effective mass of both contact partners $m^* = (1/m_p + 1/m_w)^{-1} \approx m_p$. Note that we use index *p* for the particle and index *w* for the wall.

The Hertzian constant k'_{el} in Eq. (5) can be given by the following expression:

$$k'_{el} = \frac{2}{3} E^* \sqrt{R^*}, \tag{6}$$

with the median radius of contact partners $R^* = (1/R_p+1/R_w)^{-1} \approx R_p$, by $R_W \rightarrow \infty$. The energy dissipation in the contact model is controlled by a damping parameter $_d$ which depends on the restitution coefficient. The restitution coefficient and Hertzian constant can be obtained experimentally using compression and free-fall tests [12]. The modulus of elasticity E^* of contact partners ($E_w >> E_p$, $E_w \rightarrow \infty$) is given as [12]:

$$E^* = 2\left(\frac{1-\nu_p^2}{E_p} + \frac{1-\nu_w^2}{E_w}\right)^{-1} \approx \frac{2E_p}{1-\nu_p^2}, \tag{7}$$

where is the Poisson ratio.

The viscous resistance arises during particle movement in the liquid due to the liquid shear flow between granule and wall. For a Newtonian fluid the viscous force F_{vis} was found as [10], [11]:

$$F_{vis} = \pm \frac{6\,\pi\,\eta\,R_p^2}{h_s - x}\frac{dx}{dt}, \tag{8}$$

where $\eta$is the viscosity of the liquid and (h_s-x) is the separation distance between the particle and the wall.

The capillary force in the liquid bridge depends on the Laplace hydrostatic pressure difference across the fluid surface and on the cross-section area of the neck:

$$F_{cap} = -\gamma_{la}\left(\frac{1}{R_1} - \frac{1}{R_2}\right)\pi R_p{}^2 \sin^2\alpha, \tag{9}$$

where R_1 and R_2 are the local radii of the curvature (Fig. 2). Here a minus is written before the radius R_2 due to concave meridional curvature of the bridge.

The gravitational force $F_{l,g}$ in Eq. (1) considers the mass of a liquid film which moves with the particle in the last period of impact. However, as it will be shown later this force is small in comparison with other forces and can be neglected.

The energy loss $E_{diss,tot}$ during particle collision can be described using the restitution coefficient e_n which is equal to the square root of the ratio of elastic energy $E_{kin,R}$ released during the restitution to the initial kinetic impact energy E_{kin} [13]:

$$e_n = \sqrt{\frac{E_{kin,R}}{E_{kin}}} = \sqrt{1 - \frac{E_{diss,tot}}{E_{kin}}} = \frac{|v_R|}{v}. \tag{10}$$

2. TESTING METHOD AND MATERIALS

2.1 Free-fall apparatus

Fig. 3 illustrates the used experimental free-fall setup. Before the granule is dropped, it is being held at a predetermined height *h* above the target with the aid of a vacuum nozzle that releases the granule with zero initial velocity and rotation. The different material of the target (glass and steel flat walls) was tested.

From Eq. (10) it follows that the normal restitution coefficient is a ratio of relative rebound velocity v_R (at the bridge rupture) to that before the impact v (at the contact with the liquid).

These velocities were obtained from normal impacts captured using a high-speed video camera with a frequency of 7000 frames per second.

A polymer ring film attached to the target surface formed the borders for the liquid layer. The viscosity of the liquid film was varied by adding different amounts (3-10 % w/w) of hydroxypropyl methylcellulose (HPMC, Pharmacoat® 606 from Shin-Etsu Chemical Co. Ltd., Tokyo) and maltodextrin to the water. The impact behavior was studied by varying the viscosity of the liquid layer between 1 and 300 mPas and for a thickness of the liquid layer between 40 μm and 1000 m.

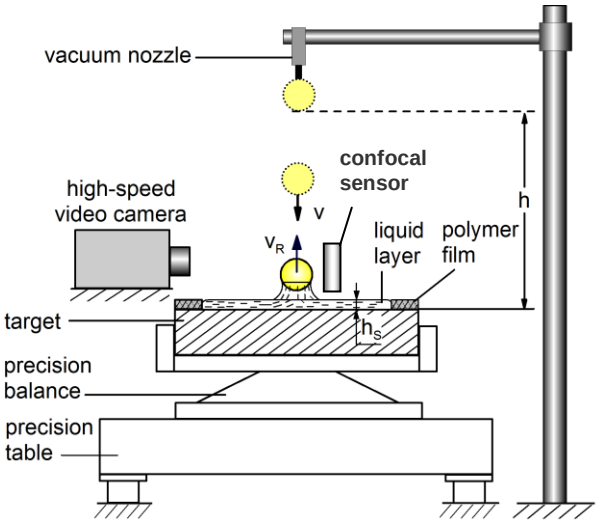

FIGURE 3. The free-fall device for investigating granule impact on a wall which is covered with a liquid layer.

2.2 Measurement of the liquid thickness

During the experiments the mass and the height of the liquid layer decreased due to the evaporation of the water. Thereby the viscosity of the solution increased corresponding to the water content in the solution. The liquid thickness at the impact, i.e. current hight of the liquid film, was measured by two different ways: direct measuring with a confocal displacement sensor and weighting using a precision balance.

A confocal displacement sensor was installed close to the impact point on the liquid surface (Fig. 3). The confocal sensor produces the polychromatic light. The lenses of sensor break down the light by controlled chromatic aberration into monochromatic wavelengths dependent on the displacement or distance between the sensor and the target. The target or the liquid layer surface reflects the light. It is detected by the receiver of the sensor which processes the spectral changes. The separation distance between the wall and the sensor, which was constant during the experiments, was measured to calculate the current thickness of the nontransparent liquid film as the difference between both distances. This sensor can obtain the distance to the liquid layer surface with a resolution of 1 μm.

The ambient temperature was 24 °C. The liquid film surface area on the target was 17.64 cm^2. The typical evaporation curves for two water layers of different initial heights and a maltodextrin solution are shown in Fig. 4. The evaporation of the water layer is about seven times faster than for the used aqueous maltodextrine solution with gradients in the range of 0.13-0.17 μm/s for water and 0,020-0.024 μm/s for the maltodextrine solution.

Additionally, the decrease of the mass of the liquid layer can be explained by liquid transfer to the particle during impact. Liquid is not only absorbed at the surface of the granules but will also penetrate into the supra-molecular and capillary structure

of the particles. Therefore the liquid mass was measured before each test to obtain the

current height and viscosity of the layer. This measurement was carried out with the help of a precision balance on which the target was placed.

2.3 Studied materials

The ballotini glass particles (d = 2.5-2.8 mm, nonporous, density of 2490 kg/m^3), -Al_2O_3 granules (d = 1.7-1.9 mm, pososity of 69 %, density of 1040 kg/m^3) and agglomerates of maltodextrin (d = 2.0-3.0 mm) were chosen as test materials. The maltodextrin agglomerates were produced by agglomeration of a maltodextrin powder (Cerestar/F) in a fluidized bed. The maltodextrin had a dextrose-equivalent (DE) in the range of 17 to 20.

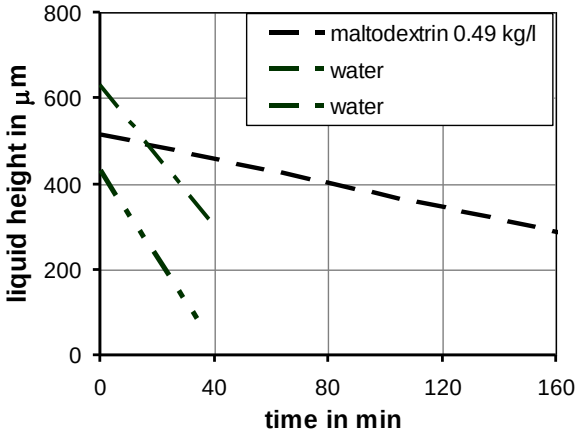

FIGURE 4. Evaporation kinetic the used water and maltodextrin solution films (at the temperature of 24° C, relative air humidity of 48 %, air velocity of about 5 mm/s, laminar airflow).

3. EXPERIMENTAL RESULTS OF RESTITUTION COEFFICIENT

To obtain the "dry" restitution coefficient the free-fall experiments were carried out without the liquid layer on the target. Fig. 5 shows the "dry" restitution coefficient depending on the impact velocity. The glass particles showed the dominantly elastic impact behaviour, the -Al_2O_3 granules behave elastic-plastically and the maltodextrin is dominantly plastic in the examined velocity range.
Only for -Al_2O_3-granules the increasing impact velocity in the examined range does not change the mean coefficient of restitution. In other words, these granules exhibit elastic-plastic behaviour without a viscous effect during the impact in this velocity range. The glass and maltodextrin showed a viscous effect.
The impact on the steel wall is more plastic then on the glass wall. The following mean restitution coefficients at impact velocity v = 1 m/s were obtained: $e_n = 0.97 \pm 0.01$ for the impact glass particle - steel wall and e_n = by 0.88 ± 0.03 for the glass particle - glass wall.

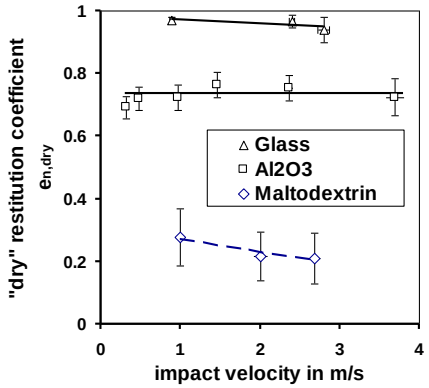

FIGURE 5. Influence of the impact velocity on "dry" restitution coefficient of investigated particles: glass particles - glass wall, -Al_2O_3-granules - steel wall, maltodextrin agglomerates - glass wall.

The experimental results (Fig. 8) showed that the decrease of the impact velocity could greatly reduce the restitution coefficient of -Al_2O_3 granules and the layer height required for adhesion. This experimental fact is also confirmed by trials using glass particles (Fig. 9). Therefore, a smaller restitution coefficient is caused by the longer time for energy absorption during penetration in the layer and stretching of the bridge. In contrast to wet conditions, the restitution coefficient of -Al_2O_3 granules for the impact on a dry and not wetted target is independent of velocities in the range of 0.5-4.5 m/s (Fig. 5).

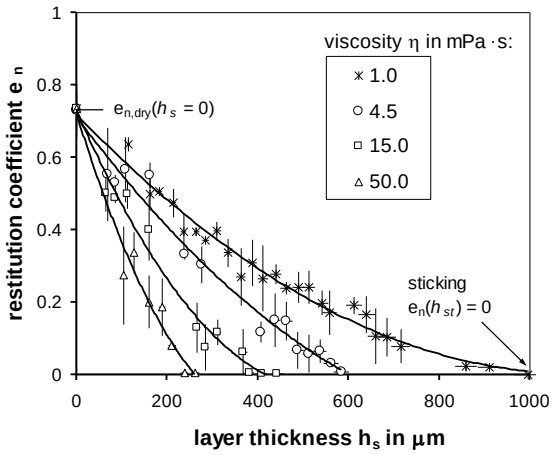

FIGURE 6. Influence of viscosity and thickness h_s of the liquid layer (aqueous solution of HPMC) on the restitution coefficient of -Al_2O_3 granule - steel wall (v = 2.36 m/s).

The results of free-fall tests for -Al_2O_3 granules are shown in Fig. 6. The restitution coefficient becomes smaller with increasing thickness and viscosity of the liquid layer, when the amount of absorbed energy increases. The maximum of the restitution coefficient ($e_{n,dry}$) corresponds to the impact without the liquid layer. The minimum of the restitution coefficient equals to zero which means the granule sticks to the target. The corresponding layer thickness h_{st} depends on the viscosity and the impact velocity. With larger liquid viscosity the layer thickness required for sticking decreases (see Fig. 7). Thus, to increase the agglomeration rate of particles, either the viscosity or the thickness of the binder layer should be increased.

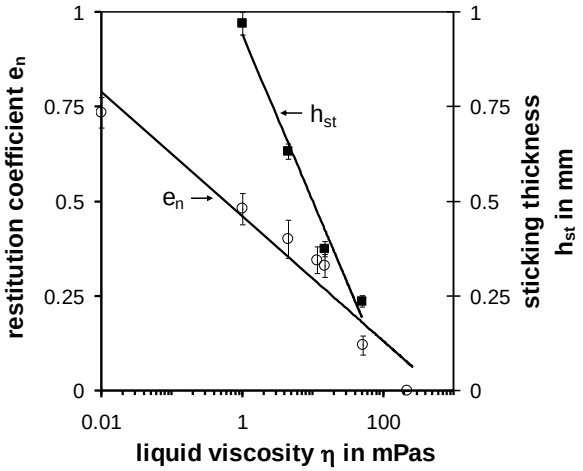

FIGURE 7. Effect of liquid viscosity on the restitution coefficient e_n of -Al_2O_3 granule - steel wall (layer thickness of 200 m, aqueous solution of HPMC) and on the layer thickness h_{st} required for adhesion.

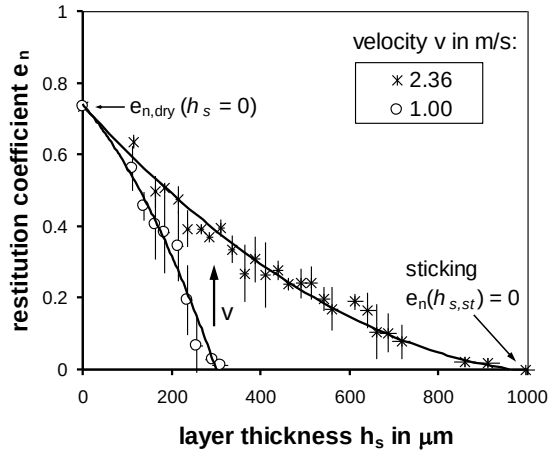

FIGURE 8. Influence of the impact velocity on the restitution coefficient of γ-Al_2O_3 granules impacting on a water layer on the steel-wall.

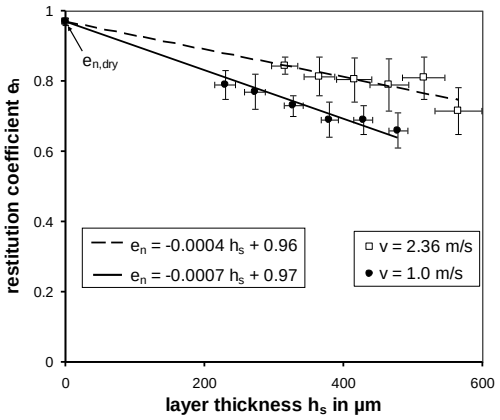

FIGURE 9. Influence of thickness h_s of the water layer on restitution coefficient of the glass particle - glass wall at different impact velocity v.

4. SIMULATION results

The numerical calculations of the equation of motion (1) were performed for the impact of γ-Al_2O_3 granules impacted at the velocity of 2.36 m/s on the steel wall with a liquid layer of viscosity = 4.5 mPa·s, which correspond to the conditions of the performed free-fall experiments. The damping parameter α_d was assumed to be 0.23 according to the restitution measured coefficient. Using Eq. (6) the Hertzian constant k'_{el} in Eq. (7) was calculated from modulus elasticity E_p = 14.6 GPa [12] by 592 MN/$m^{1.5}$.

In Fig. 10 the experimentally obtained and calculated restitution coefficients at different liquid layer thicknesses are compared with each other. A good agreement of the calculated values with the experimental data can be observed.

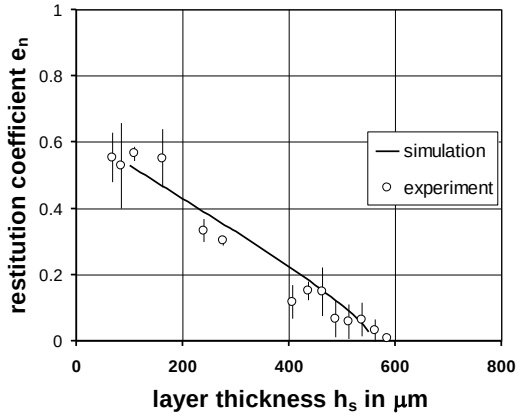

FIGURE 10. Experimental and calculated normal restitution coefficients versus liquid layer thickness (η = 4.5 mPa·s, γ_{la} = 43.6 mN/m, Θ_R = 25°, Θ = 175° and v = 2.36 m/s).

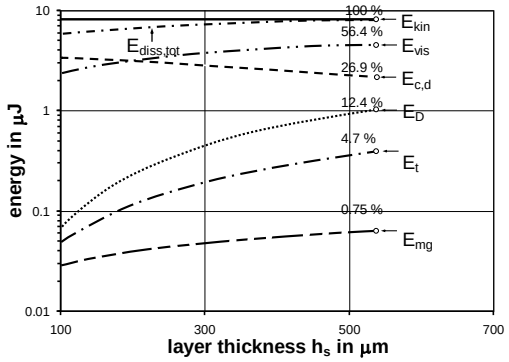

FIGURE 11. Kinetic impact energy (v = 2.36 m/s) and dissipated energy parts versus liquid layer thickness (η =4.5 mPa·s). The plotted values show the contribution of different energies at the sticking point. (E_{kin} initial kinetic energy of the impacted particle, $E_{diss,tot}$ - total energy dissipation, E_{vis} - viscous energy dissipation and E_D - energy dissipated due to drag forces, E_t - energy dissipated due to surface tension, E_{mg} - energy dissipated due to gravitation forces of particle and liquid remained on the particle after the rebound.)

Fig. 11 shows the influence of different forces on the total energy dissipation ($E_{diss,tot}$), which increases with the layer thickness and equals the initial kinetic energy (E_{kin}) at the sticking point. Viscous (E_{vis}) and drag forces (E_D) are having the biggest impact on the energy absorption during penetration and rebounding. Hence, the drag force is significantly influencing the process only at thick layers ($h_s/R_p > 0.3$). The surface tension (E_t) should also be considered in the case of small liquid viscosities and particle velocities when the contribution of the drag and viscous forces become smaller. The energy loss due to deformation ($E_{c,d}$) has the same order of magnitude as the viscous energy dissipation.

REFERENCES

1. M. S. van Buijtenen, N. G. Deen, S. Antonyuk, S. Heinrich and J.A.M. Kuipers. The Canadian Journal of Chemical Engineering, 87(2), pp. 308-317.
2. P. Müller, S. Antonyuk, J. Tomas and S. Heinrich. In Micro-Macro-Interactions in Structured Media and Particle Systems, Springer, Berlin, 2008, pp. 235-243.
3. B. Ennis, G. Tardos and R. Pfeffer. Powder Technology 65, 1991, pp. 251-272.
4. F. M. Orr, L. E. Scriven and P. Rivas. J. Fluid Mech. 67, 1975, pp. 723-742.
5. H. Schubert. Powder Technology 37, 1984, pp. 105-116.
6. C. D. Willet, M. J. Adams, S. A. Johnson and J. P. K. Seville. Powder Technology 130, 2003, pp. 63-69.
7. A. A. Kaskas. Doctoral dissertation, Technical University of Berlin, 1970.
8. S. Antonyuk. Doctoral dissertation, University of Magdeburg, 2006.
9. Y. Tsuji, T. Tanaka and T. Ishida. Powder Technology 71, 1992, pp. 239-250.
10. A. Cameron. “Basis lubrication theory”, Ellis Harwood, Chichester, 1981.
11. G. Lian, Y. Xu, W. Huang and M. J. Adams. J. Non-Newtonian Fluid Mech. 100, 2001, pp. 151-164.
12. S. Antonyuk, S. Heinrich, J. Tomas, N. G. Deen, M. S. van Buijtenen and J. A. M. Kuipers. Granular Matter, 2009, in press.
13. W.J. Stronge, (2000). Cambridge University Press.